Hindawi
Shock and Vibration
Volume 2023, Article ID 2227785, 13 pages
https://doi.org/10.1155/2023/2227785

Research Article

Dynamic Numerical Simulation Model and Time-Domain Identification of Flexible AERORail Structure

Fang-yuan Li,[1] **Zhen-wei Guo**,[1] **Yun-xuan Cui**,[2] **and Si-hang Wei**[3]

[1]*Department of Bridge Engineering, College of Civil Engineering, Tongji University, Shanghai 200092, China*
[2]*School of Civil and Environmental Engineering, University of New South Wales, Sydney, NSW 2052, Australia*
[3]*Jujie Technology Development Group Co. Ltd., Ningbo 315615, China*

Correspondence should be addressed to Fang-yuan Li; fyli@tongji.edu.cn

Received 17 December 2022; Revised 15 May 2023; Accepted 3 June 2023; Published 12 June 2023

Academic Editor: Lutz Auersch

A simplified theoretical model of the AERORail vehicle-bridge coupling system and a corresponding numerical simulation system in Simulink are established. Based on several widely used methods for modelling and simplifying vehicle systems, the Simulink simulation system used in this study, including the vehicle system and the bridge (AERORail) system, is presented. Identification examples using a moving load model and a simplified 1/4-scale vehicle model are established. The simulation results agree with the data of the simplified dynamic model, with errors between 2.9% and 4.72%, and a satisfactory accuracy is achieved even for single-point signal identification, thereby verifying the correctness of the simplified dynamic model of the AERORail system and the improved time-domain method based on the method of moments.

1. Introduction

The AERORail transportation system, referred to as AERORail, is a new type of cable-rail composite structure consisting of multispan continuous chord cables, rails, lower supports, and related power and control systems [1] and is somewhat similar in appearance to existing cable-supported suspension bridges (Figure 1). However, in contrast to traditional bridges, the AERORail structure uses steel as the structural material instead of concrete and prestressed concrete (PC) for the superstructure, eliminates the heavy bridge deck in traditional bridges, and forms a spatial force-resisting system by directly using the steel rail and the chords together. The structural stiffness is mainly derived from the stress stiffness formed by the pretensioning of the chord cables, and the system exhibits the obvious characteristics of a flexible structure.

Traditional light rail systems often require the construction of heavy girders to carry the rail and vehicles, such as the PC rail girders and steel box rail girders used in the Chongqing light rail [2], the PC channel girders used in the Shanghai rail transit system, and the German-made suspended sky train planned for introduction in Ningbo [3].

Compared with the abovementioned traditional structures, AERORails have the advantages of a simple structural form, low construction cost, less resource consumption, fast construction speed, and low impact on the environment. In view of the large proportion of steel structure in AERORails and the need for concrete and earthwork only for the foundation, these systems can be constructed at a fast pace with relatively little pollution to the environment. Moreover, the superstructure of an AERORail occupies only a small space, and its structure is completely hollowed out and easy to see through; hence, it has little impact on the natural or urban landscape. Therefore, AERORails have significant advantages in terms of environmental protection.

Research on the AERORail structure has mainly focused on its static and dynamic behaviour. Researchers at Tongji University preliminarily verified the feasibility of the AERORail structure using 1 : 20 and 1 : 15 scale models and used a virtual prototype to investigate the dynamic and static behaviour of the structure [4, 5]. They conducted numerical

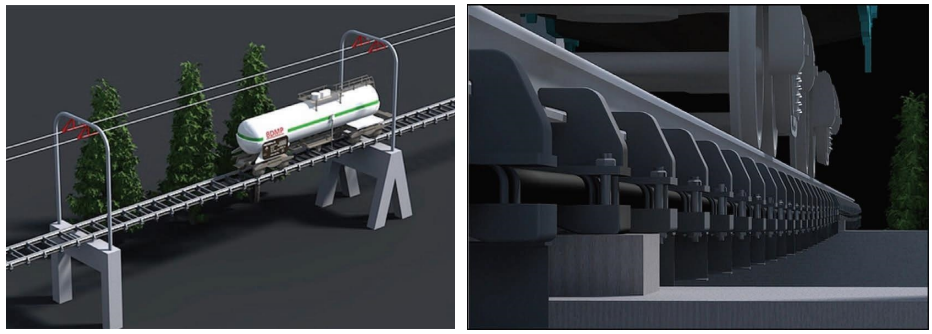

Figure 1: Schematic diagram of an AERORail transportation system.

analysis on the static deflections of AERORails with different spans under different loads and pretensions and experimentally verified the numerical results using a 1 : 1 full-scale AERORail model. On this basis, they investigated the dynamic deflection responses of AERORails with different spans using vehicle-bridge coupling theory.

Studies have demonstrated that the cable stress increment, dynamic deflection, and structural stiffness of the AERORail structure do not change significantly under low-speed moving loads, that the structural stiffness increases significantly with increasing cable force and midspan support height, and that there is a nonlinear relationship between vehicle speed and dynamic deflection [4, 5]. Although these studies have preliminarily revealed some of the static and dynamic characteristics of the AERORail structure, their results are still inadequate for the further development of related research and engineering applications.

In practical engineering, the consideration and selection of loads are the first and also one of the most important steps in designing a structure. Static loads are often determined based on statistical data from field investigations and using a safety factor to ensure a certain level of structural performance [6]. Dynamic loads, including moving loads and dynamic loads in the narrow sense, come from effects of the external environment on the structure, such as wind, an earthquake, or an explosion. These effects are collectively referred to as the external excitation. The dynamic response of a structure, including its acceleration, velocity, and displacement, is the result of the interaction between the structure's own properties and the external excitation. In some cases, the structure has little effect on the excitation (e.g., earthquake), but there are many cases of coupling (e.g., wind-induced vibration and wave action), for which the research often has a high degree of complexity. Compared to the traditional problem of finding the vibrational response with known structural parameters and external excitations, the study of excitation, especially the calculation of excitation based on existing responses and structural parameters, is an inverse problem that emerged late in the study of vibration systems, i.e., the dynamic load identification problem.

Dynamic load identification technology was initially developed in the 1970s and was first used for military purposes. Currently, the mainstream dynamic load identification methods include time-domain methods (TDMs) and frequency-domain methods (FDMs). FDMs are based on the Fourier transform or the Laplace transform. By establishing a transformation relationship between the excitation and response in the frequency domain (such as the frequency response function), the corresponding excitation can be calculated from the measured response. FDMs were studied earlier and are relatively mature, but they impose a requirement on the sample length of the response signal (it must usually be longer than a specified length). Therefore, FDMs are generally used only for stationary random loads or steady-state dynamic loads [7]. TDMs are usually based on the kinetic equations of the system. By inverting the convolution integral of structural responses, the dynamic load applied to the structure is determined throughout the time. The responses used in identification can be displacement, velocity, and acceleration. Some classic methods in the time domain are the deconvolution method, weighted acceleration method, and function fitting method [8, 9]. In recent years, a series of new methods have also been reported, such as time finite element methods, inverse system methods, neural network-based methods, and transformation with orthogonal wavelet operators [10]. In contrast to FDMs, TDMs are sensitive to boundary conditions and initial values, but they can be used for nonlinear systems and to identify transient impact loads [11, 12], and their identification accuracy is not influenced by the signal acquisition method [13, 14]. Additionally, TDMs can capture the actual history of time-dependent loads at each specific time increment. This history of load usually has a clear physical meaning and is therefore more practical to guide the design and improvement of AERORail structure.

In bridge engineering, there is another branch of dynamic load identification—moving load identification. In contrast to general dynamic load identification, moving load identification mostly involves vehicles traveling on bridges. It is very important to determine the dynamic effect of moving vehicles on the structure in bridge design and construction. However, because the interaction between the two is closely related to the design parameters of the bridge, the design parameters of the vehicles, and the driving speed, the force between each vehicle and the bridge is often difficult to quantify accurately. Therefore, it is necessary to calculate the force between each vehicle and the bridge using the dynamic load identification method [15]. A very prominent feature of moving load identification is that the

action point of the external excitation changes with time. As a result, some traditional methods for dynamic load identification, such as frequency response function inversion, cannot be directly applied to moving load identification. Based on the advantages of TDMs, we use a time-domain method which is improved by the method of moment to identify the contact force between the vehicle and the structure.

To verify whether the improved time-domain method (ITDM) can capture the dynamic load applied on the structure, a simplified structure-vehicle model is used in the test case. This simplified model is a system of partial differential equations (ODE) containing both the vehicle and the structure's kinetic equations, where the structural and material parameters of AERORail are utilized. The solution of this system is obtained by Simulink.

The article is structured as follows: Section 2 proposes a system of ODEs as a simplified structure-vehicle model, which is used in the next section for verification. The numerical procedures to solve the equations are also introduced therein. The theory and numerical implementation of ITDM are briefly explained in Section 3. To fully investigate ITDM's ability of capturing the dynamic external load, two test cases with a moving force and a ¼ vehicle model are presented in Section 4. The summary of main conclusions of this study is provided in Section 5.

2. Simplified Dynamic Numerical Model of an AERORail System

The joint vibration effect of vehicle and bridge structures, i.e., vehicle-bridge coupled vibration, is an important property in bridge structural dynamics. In engineering practice, usually due to the limitations of the calculation method and time cost, only the vibration of the bridge itself is considered, or each vehicle is simplified as a moving mass block in structural analysis and verification, which clearly fails to fully and truly reflect the effect of vehicle-bridge coupled vibration. Generally, to comprehensively consider the vehicle-bridge coupled vibration problem, the vehicle dynamics, rail dynamics, and wheel-rail contact relationship should be considered and analysed as a whole coupled system. To this end, Hwang and Nowak [16], Wang and Huang [17], Yang et al. [18, 19], Tan et al. [20], and Kwasniewski et al. [21] proposed numerical vehicle-bridge coupling models based on beam elements, plane bar systems, or solid simulation models, which gradually achieved results with satisfactory accuracy and were relatively consistent with experimental results.

In these vehicle-bridge coupling models, there are four vehicle model options (Figure 2).

(1) *The Moving Mass Model* (Figure 2(a)). The calculated midspan deflection of the bridge is relatively large and can reflect the vibration of some vehicles and bridges;

(2) *The 1/4-Scale Vehicle Model* (Figure 2(b)). This model increases the fluctuation of the deflection response relative to the moving mass model, and the calculation results of the two models are similar.

(3) *The 1/2-Scale Vehicle Model* (Figure 2(c)). The calculated maximum deflection is relatively small, and the deflection results fluctuate greatly.

(4) *The Full Vehicle Model* (Figure 2(d)). This model generates accurate results and can represent the vibration effect caused by "swaying motions" and "nodding motions," but its calculation is complex and costly.

Notice that in the rest of the paper, the coordinate system of the beam is along its axis with the origin at the end where the load/vehicle makes the first contact with the beam.

There are some assumptions shared by these vehicle models:

(1) The friction force between wheels and the structure is ignored. This is mainly because the deflection is a major concern in structural safety; therefore, the vertical load is what engineers care more about.

(2) The kinematics of vehicle systems does not take ambient vibrations (for example, vibration from the motor) into account.

(3) The parameters assigned to the systems are from numerical analysis or an investigation of the literature. There could be the difference between these chosen parameters and the real properties of the structure.

For the dynamic load identification problem considered in this study, the full vehicle model and the 1/2-scale vehicle model are too complex, the 1/4-scale vehicle model is appropriate, and the moving mass model is computationally simple and can be used as a simplified model for practical calculation. In the following, the simplified 1/4-scale vehicle model and the moving load (ML) model are used to calculate the vehicle-bridge coupled vibration of the AERORail structure using modal decomposition. Then, this numerical simulation system is used to verify the improved TDM (ITDM) based on the method of moments.

2.1. Simplified Dynamic Numerical Model of the AERORail Structure. It is assumed that a vehicle moving on the AERORail structure can be simplified as a vibration system composed of masses, springs, and dampers. Taking the single-degree freedom system as an example, the vibration equation can be expressed as the following equation:

$$m_c\ddot{w}_c + c_c\dot{w}_c + k_c(w_c - w(ct)) = f_{ct} - m_c g, \quad (1)$$

where m_c, c_c, and k_c are the mass, damping, and contact stiffness, respectively, of the simplified vehicle system; w_c is the vertical displacement of the centre of mass of the simplified vehicle system relative to the geodetic coordinate system; $w(ct)$ is the deflection of the bridge at the coordinate ct at time t, where c is the moving speed of the vehicle system; f_{ct} is the contact force between the vehicle system and the bridge system; and $m_c g$ is the gravitational force on

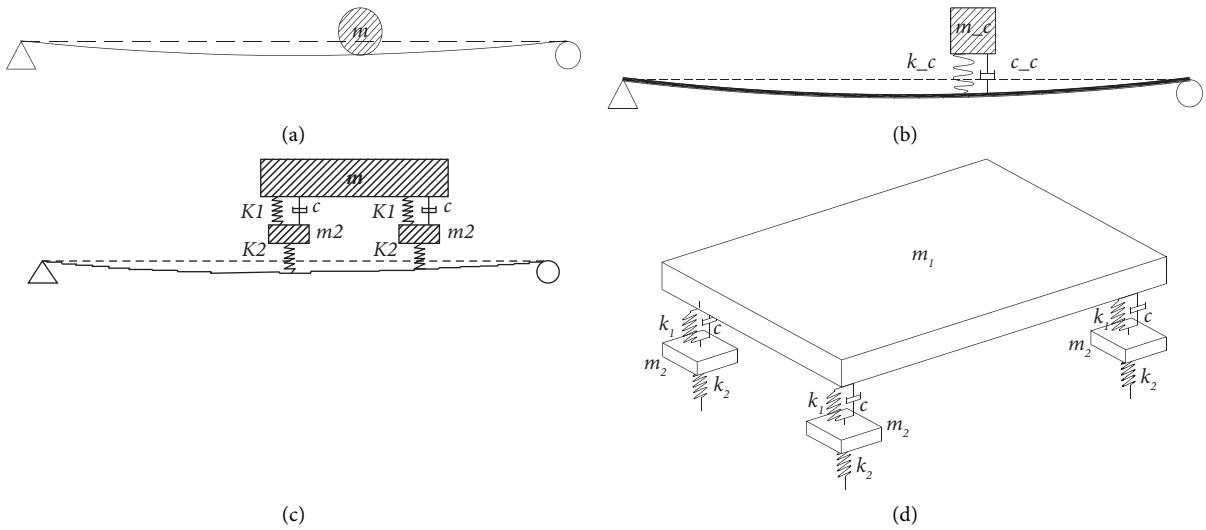

Figure 2: Four vehicle model options. k_i, m_i, and c_i represent the springs, masses, and dampers in a kinematic system, respectively. (a) Schematic diagram of the moving mass mode. (b) Schematic diagram of the 1/4-scale vehicle model. (c) Schematic diagram of the 1/2-scale vehicle model. (d) Schematic diagram of the full vehicle model.

the vehicle system. The corresponding vibration equation of the bridge structure can be expressed as the following equation:

$$\ddot{q}_n + 2\xi_n\omega_n\dot{q}_n + \omega_n^2 q_n = \frac{2}{\rho_b L_b}\sin\left(\frac{n\pi ct}{L_b}\right)f_{ct}, \tag{2}$$

where q_n is the modal displacement, ξ_n is the modal damping ratio, ω_n is the modal circle frequency, $\rho_b\, b$ is the linear mass of the beam, L_b is span, and n is the order. Notice that the bridge structure here is assumed to be an Euler-Bernoulli beam.

The above two equations and their parameters together form a simplified dynamic numerical model of the AERORail. The vibration differential equations of this coupled system can generally be solved using the Newmark-β and Wilson-θ methods. In this study, Simulink is used to build a simulation system of the model, and the ode45 solver is employed to solve the equations using the 4/5th-order Runge–Kutta method.

2.2. Calculation Module of the Vehicle System. To build a calculation module using Simulink, it is necessary to first change the vibration differential equation into a form that can be directly calculated by the integrator, that is, an explicit expression of acceleration. By slightly rearranging terms in equation (1), we obtain

$$\ddot{w}_c = \left(\frac{1}{m_c}f_{ct} - g\right) - \left(2\xi_c\omega_c\dot{w}_c + \omega_c^2\left(w_c - w(ct)\right)\right). \tag{3}$$

The constant parameters in equation (3) that must be determined in advance are ξ_c, ω_c, m_c (or m_c, k_c, and ξ_c), c and g, where g is the acceleration of gravity. The deflection of the contact point, $w(ct)$, must be "input" from the outside continuously to calculate the contact force, f_{ct}, which is "output" continuously. The calculation module of the vehicle system in Simulink is shown in Figure 3.

To make the vehicle system enter the bridge structure "smoothly," it is necessary to eliminate the transient vibration of the vehicle system caused by gravity at the beginning of the calculation. To this end, the following initial integration condition is introduced into the integrator:

$$w_c\big|_{t=0} = \frac{m_c g}{k_c}. \tag{4}$$

To simulate multivehicle or multiwheels conditions, it is only necessary to make multiple copies of this module and connect them to the calculation process.

The contact force in Figure 3 is an interface to the AERORail calculation module, in which the location and the value of the load are the current coordinate and the contact force of the vehicle. Notice that the contact force itself as an unknown is solved together with other variables in the Simulink using an explicit solver.

2.3. Calculation Module of the AERORail System. The modal acceleration of the bridge structure, i.e., the AERORail structure, is expressed as follows:

$$\ddot{q}_n = \frac{2}{\rho_b L_b}\sin\left(\frac{n\pi ct}{L_b}\right)f_{ct} - \left(2\xi_n\omega_n\dot{q}_n + \omega_n^2 q_n\right), \tag{5}$$

where the constant input parameters are ρ_b, L_b, c, ξ_n, and ω_n. The contact force f_{ct} is obtained from the vehicle system calculation module. The single-mode vibration calculation module of the AERORail system in Simulink is shown in Figure 4.

The module in Figure 4 is a single-mode vibration calculation module. Because the multimode vibration response must be calculated in the simulation, it is necessary to

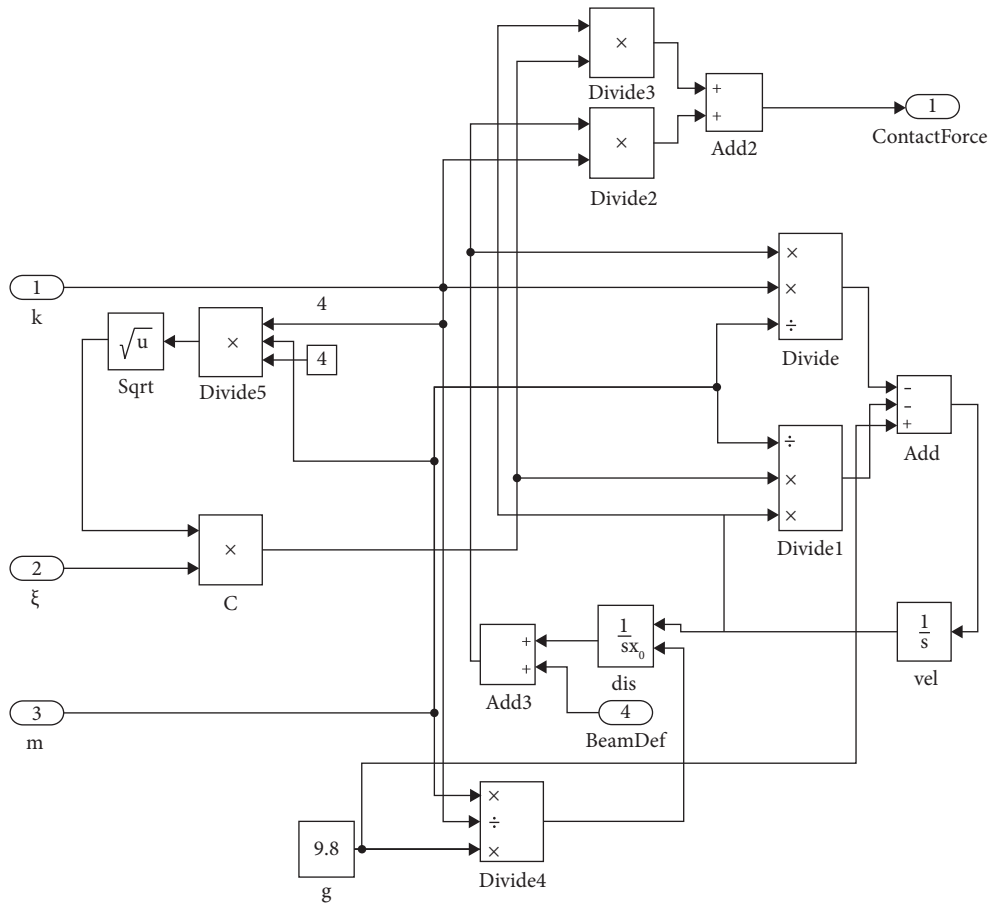

Figure 3: Schematic diagram of the Simulink calculation module of the vehicle system.

make multiple copies of this module according to the required number of modes and call them in parallel in the calculation.

The locs and $f(t)$ in the AERORail calculation module are the current coordinates and values of the excitation force. For example, when vehicle module is linked to the system, locs1 and $f(t)1$ are the coordinates and contact force (see Figure 3) of the first ¼ vehicle model. The vehicle's coordinates are taken care of by an overall control unit which evaluates locs1 = ct at every simulation instance. Moreover, in the moving load example, the $f(t)1$ is not an unknown but a known function predefined by the user.

Since the structural modes are used in the ODE, the structural responses at certain points, such as deflections, speeds, and accelerations, are recovered from the simulation results using the amplitudes of all structural modes involved in the simulation.

3. ITDM Based on the Method of Moments (MoM)

TDMs for identification exhibit instability in practical identification, which is mainly reflected in the large size and severe ill-conditioning of the solution matrix [22–24]. In the area of antennas, microwaves, and electromagnetic waves, the method of moments is a widely accepted tool to address this issue. As a long-established procedure in the statistics, the method of moments provides a good estimation that matches the true and sample moments. Since the mathematics of inversing the convolution integral equations are replaced by statistic estimation, the algorithm's stability and the solution's quality are significantly improved.

We present here a brief introduction to the MOM $[A]$ for an inhomogeneous equation as follows:

$$D(f) = g, \tag{6}$$

with L, g, and f being the linear operator, a known forcing function, and an unknown function, respectively. Given a set of basis functions f_n that are nearly independent, an approximate solution of f can be expressed as follows:

$$f = \sum_{n=1}^{N} a_n f_n, \tag{7}$$

where a_n are weighting coefficients to be determined. In a Hilbert space, the inner product of functions f and g is defined as follows:

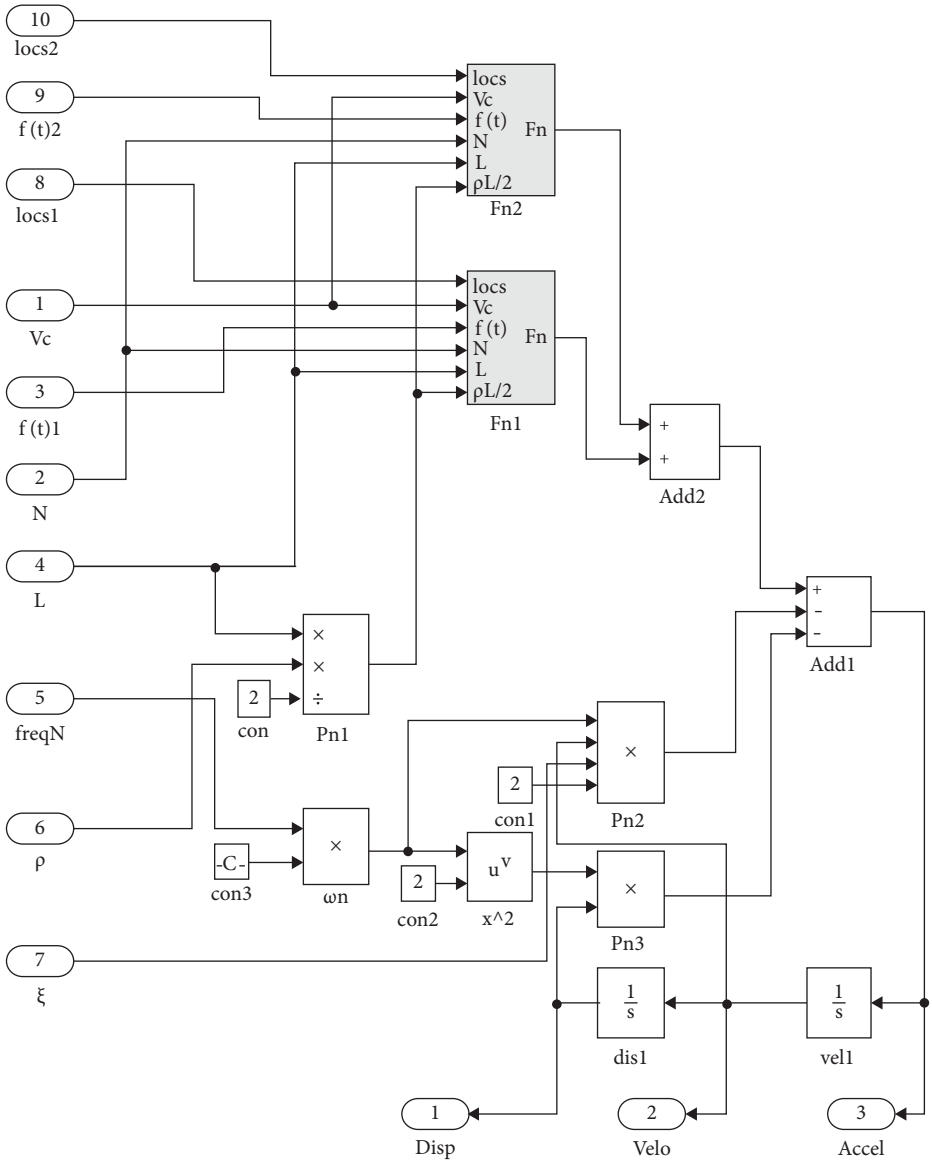

Figure 4: Schematic diagram of the single-mode vibration calculation module of the AERORail system in Simulink.

$$\langle f, g\rangle = \int_{\Omega} f \cdot g \, d\Omega. \tag{8}$$

The solution to equation (5) is obtained when the inner product of residual ε_n and M selected test functions q_m equals zero.

$$\sum_{n-1}^{N} \langle q_m, \varepsilon_n\rangle = 0, \text{for } m = 1, 2, \ldots, M,$$
$$\varepsilon_n = a_n D(f_n) - g. \tag{9}$$

Equation (9) can be written in the following matrix form:

$$\mathbf{L}\vec{a} = \vec{g},$$
$$\mathbf{L} = \begin{bmatrix} \langle q_1, L(f_1)\rangle & \langle q_1, L(f_2)\rangle & \cdots & \langle q_1, L(f_N)\rangle \\ \langle q_2, L(f_1)\rangle & \langle q_2, L(f_2)\rangle & \cdots & \langle q_2, L(f_N)\rangle \\ \vdots & \vdots & \cdots & \vdots \\ \langle q_M, L(f_1)\rangle & \langle q_M, L(f_2)\rangle & \cdots & \langle q_M, L(f_N)\rangle \end{bmatrix},$$
$$\mathbf{q} = \begin{bmatrix} q_1 \\ q_2 \\ \vdots \\ q_M \end{bmatrix},$$

$$\mathbf{f} = \begin{bmatrix} f_1 \\ f_2 \\ \vdots \\ f_N \end{bmatrix},$$
$$\mathbf{g} = \begin{bmatrix} \langle h_1, g \rangle \\ \langle h_2, g \rangle \\ \vdots \\ \langle h_M, g \rangle \end{bmatrix}, \tag{10}$$
$$\mathbf{a} = \begin{bmatrix} a_1 \\ a_2 \\ \vdots \\ a_N \end{bmatrix}.$$

The original TDM is to solve the following equations at N sampling instances of acceleration:

$$\ddot{\mathbf{w}} = \sum_{n=1}^{\infty} D_{xn} \mathbf{A}_n \mathbf{f}_{ct},$$
$$D_{xn} = \frac{2}{\rho_b L_b} \sin \frac{n\pi x}{L_b},$$
$$H_n(k) = \frac{\Delta t}{\omega_n} \ddot{h}_n(k),$$
$$S(k) = \sin\left(\frac{n\pi c \Delta t}{L_b} k\right),$$
$$\mathbf{A}_n = \begin{Bmatrix} S(1)\left(1 + H_n(0)\right) & 0 & \cdots & 0 \\ H_n(1)S(1) & S(2)\left(1 + H_n(0)\right) & \cdots & 0 \\ \vdots & \vdots & \ddots & \vdots \\ H_n(N-1)S(1) & H_n(N-2)S(2) & \cdots & H_n\left(N - N_c\right)S\left(N_c\right) \end{Bmatrix}, \tag{11}$$
$$\ddot{\mathbf{w}} = [\ddot{w}_1\ \ddot{w}_2 \vdots \ddot{w}_N],$$
$$\mathbf{f}_{ct} = \begin{bmatrix} f_{ct,1} \\ f_{ct,2} \\ \vdots \\ f_{ct,N} \end{bmatrix},$$

where $\ddot{h}_n(k)$ is the unit impulse response incurred by excitation at k-th sampling instance corresponding to the n-th mode with damping, $\mathbf{A}_n$ is a coefficient matrix corresponding to n-th structural mode, N_c is the number of sampling points to the moving force, and $\ddot{\mathbf{w}}$ is the column of accelerations samples.

Using Legendre polynomials p_i up to the N_p-th order as a set of orthogonal basis functions yields equation (13):

$$\overrightarrow{f}_{ct,j} = \sum_{i=1}^{N_p} p_i \alpha_i. \tag{12}$$

Using the Dirac function $\delta(t - t_j)$ as the test function, the resultant discrete equations of acceleration and excitation force read [25]:

$$\ddot{\mathbf{w}} = \left(\sum_{n=1}^{\infty} D_{xn} \mathbf{A_n} \right) \mathbf{f}_{ct}. \tag{13}$$

Equation (9) is the system of linear equations for the ITDM based on the method of moments. Let

$$\mathbf{B} = \sum_{n=1}^{\infty} D_{xn} A_n, \mathbf{P} = P_i\left(t_j\right). \tag{14}$$

Then, equation (9) can be simplified as follows:

$$\ddot{\mathbf{w}} = \mathbf{BP}\boldsymbol{\alpha}. \tag{15}$$

Solving it using the least squares method yields the following equation:

$$\boldsymbol{\alpha} = \left((\mathbf{BP})^T (\mathbf{BP}) \right)^{-1} (\mathbf{BP})^T \ddot{\mathbf{w}}. \tag{16}$$

An approximate solution of the moving load is obtained by substituting equations (16) into (12).

In order to investigate the weight of Legendre polynomials of different orders, we plot the values of α_i in equation (15) obtained from single-point and multipoint identifications in Figure 5.

In fact, α approaches zero when N_p is greater than a threshold value. The physical meaning of this phenomenon is that in practical calculations, using Legendre polynomials beyond a threshold order has a little influence on the calculation results. Empirically choosing an appropriate order N_p of Legendre polynomials helps improve the computational efficiency without sacrificing computational accuracy.

4. Simplified Dynamic Model of AERORail and Examples of TDMs for Identification

To verify the correctness of the ITDM based on the method of moments and to ensure that the two theories are consistent and the calculations are properly connected, two identification examples are given in this section with moving loads (ML) and a simplified 1/4-scale vehicle model [26].

Moving loads model is probably the simplest case in the realm of load identification. However, it is very useful when validating algorithms and corresponding implementations, since the input is clearly defined. The ¼-scale vehicle model is adopted to test the method's ability in a close-to-reality scenario, where the structure-vehicle interaction is the dominant effect.

The calculation process and results of these two examples are aforementioned.

4.1. Example with the ML Model. The parameters of the simply supported beam simulated in this example are shown in Table 1. The listed parameters are based on the numerical estimation of an under-construction AERORail structure.

The ML is expressed as follows:

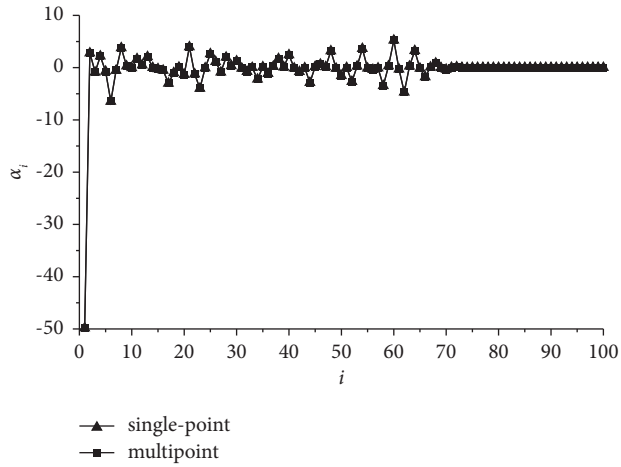

Figure 5: Relationship between α_i and i.

Table 1: Parameters of the simply supported beam in the ML model.

Parameters	ρ_b	f_1	f_2	f_3	L_b	ξ_1	ξ_2	ξ_3	c	
Units	kg/m		Hz		m	%	%	%	km/h	m/s
Values	2000	4	16	36	20	2	2	2	72	20

$$\begin{aligned} p_1 &= 50000N, \\ p_2 &= 5000\sin(4\pi t)N, \\ p_3 &= 2500\sin(15\pi t)N, \\ p_4 &= 2500\sin(40\pi t)N, \\ p(t) &= p_1 + p_2 + p_3 + p_4 N. \end{aligned} \tag{17}$$

The ML $p(t)$-t curve is plotted in Figure 6.

By substituting the load and parameters into the simplified dynamic model of the AERORail, the accelerations at the 1/4, 1/2, and 3/4 spans of the beam and the deflection at the 1/2 span of the beam are calculated, and the results are shown in Figures 7 and 8.

The acceleration curves indicate that the acceleration oscillation of the beam gradually increases as the moving load moves and gradually decreases after the load approximately passes the midspan. The deflection increases to the maximum when the moving load moves near the midspan and then gradually returns to the equilibrium position and performs free damped vibration. This calculation result is close to the actual engineering experience, indicating that the simplified dynamic numerical model of the AERORail can meet the calculation requirements to a certain extent.

The acceleration time history of the beam at the 1/2 span is used as the response sample. The signal is resampled with a frequency of $f_s = 200$ Hz and input together with the parameters of the simply supported beam of the ML model in Table 1 into the calculation program of the ITDM based on the method of moments. The calculation flow of the program is shown in Figure 9.

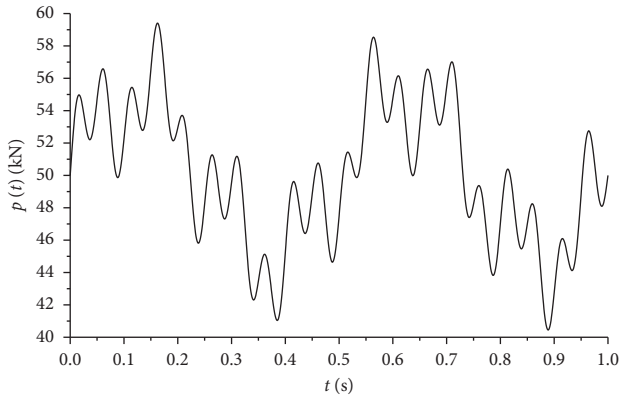

Figure 6: Time history of $p(t)$.

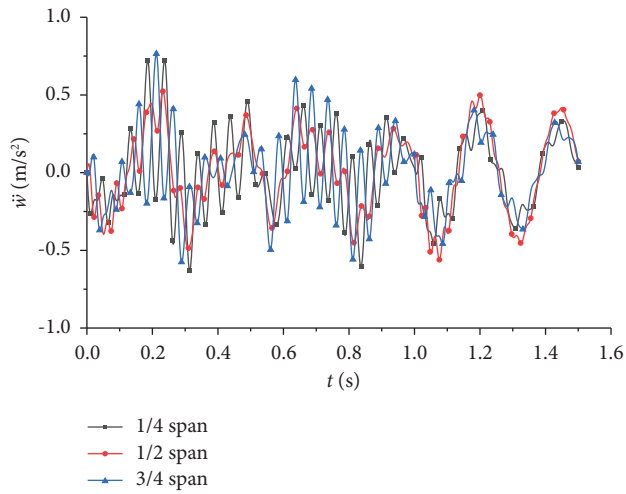

Figure 7: Time history of acceleration of the ML model.

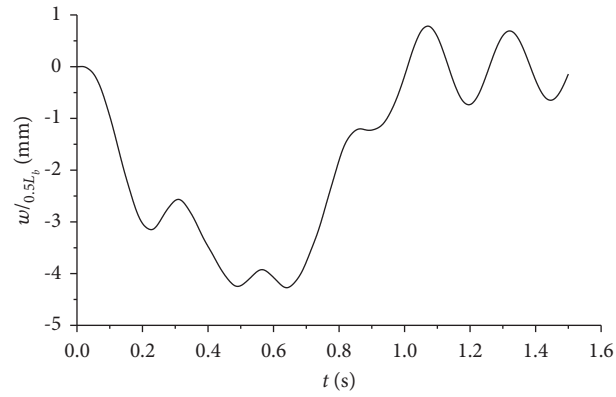

Figure 8: Time history of deflection at the 1/2 span of the ML model.

Legendre polynomials of order $m = 100$ are used in the identification calculation to obtain the identified moving load $\tilde{p}(t)$-t curve, as shown in Figure 10(a).

According to Figure 10(a), the difference between the identification result and the original result is small at the start and end time points, and the error is approximately 4.72% at the middle time point. By adding the acceleration signal at the 1/4 span of the beam as the identification input, the identification result shown in Figure 10(b) is obtained. The identification result essentially coincides with the original moving load $p(t)$-t curve, exhibiting high accuracy.

The condition number is the most commonly used metric at present to measure the degree of ill-conditioning of a matrix in engineering applications and theoretical studies

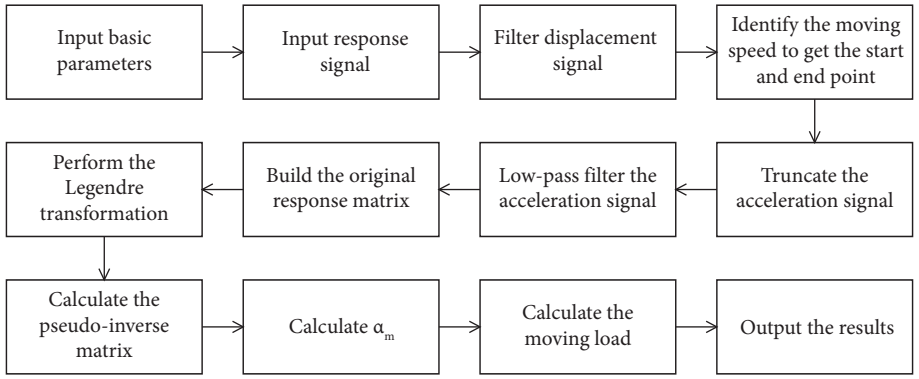

Figure 9: Flowchart of the ITDM based on the method of moments.

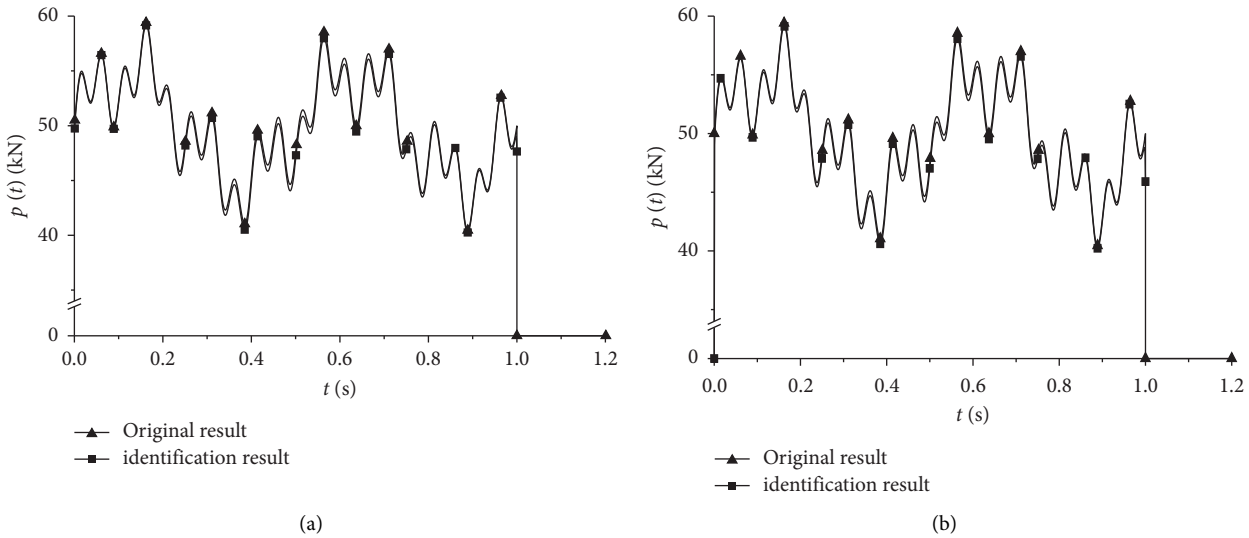

Figure 10: Time history of moving load $\tilde{p}(t)$ curve. (a) Based on single-point identification. (b) Based on multipoint identification.

Table 2: Matrix condition numbers for different identification methods.

	Single-point/original	Single-point/improved	Multipoint/original	Multipoint/improved
Unit	1	1	1	1
Condition numbers	6.15×10^{13}	2.32×10^{4}	3.51×10^{13}	1.41×10^{4}

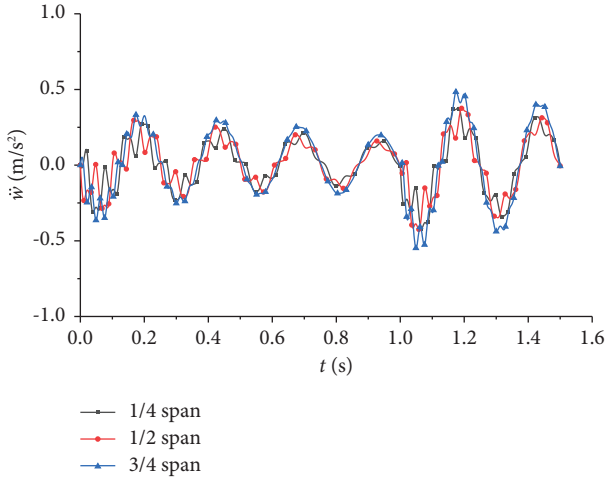

Figure 11: Time history of acceleration at different spans using the vehicle system model.

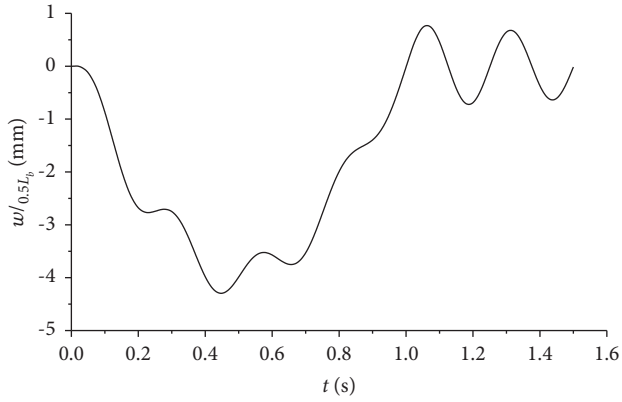

Figure 12: Time history of deflection at the 1/2 span of the beam using the vehicle system model.

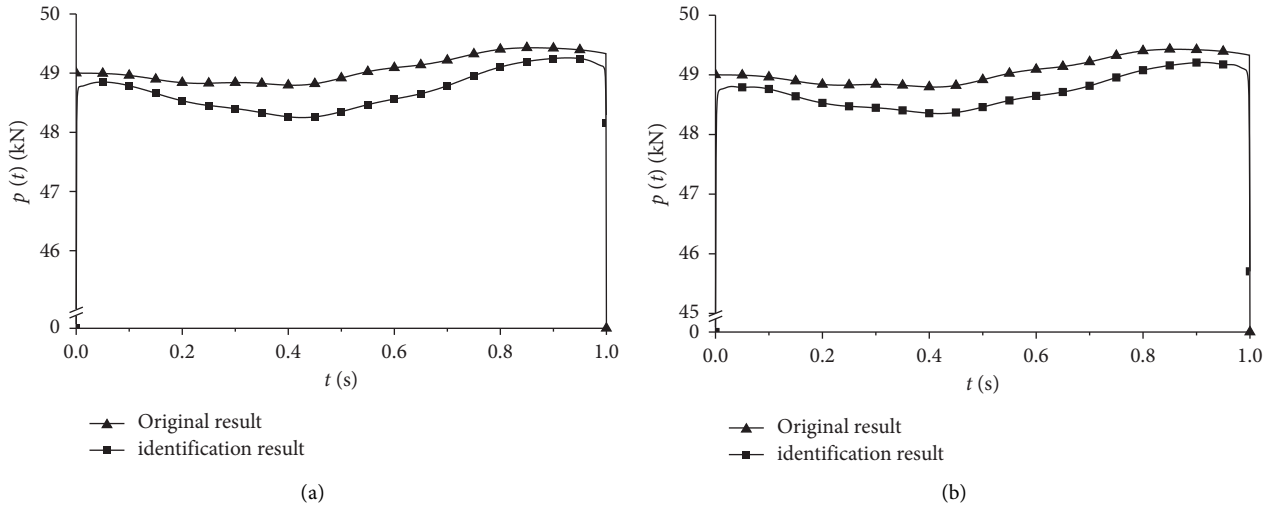

Figure 13: Moving load $\tilde{p}(t)$-t curve based on identification. (a) Based on single-point identification. (b) Based on multipoint identification.

[27]. The larger the condition number is, the closer the eigenvalue is to zero and the more severe the ill-conditioning of the matrix. To verify that the ITDM is superior to the original TDM, the matrix condition numbers in the cases of single-point identification and multipoint identification are calculated and listed in Table 2.

In 0, it was shown that the ITDM effectively reduces the matrix condition number and improves the matrix state, making the linear equations easier to solve.

4.2. Example with a Simplified 1/4-Scale Vehicle System. The parameters of the simply supported beam in this example are the same as those in the above example. The parameters of the vehicle system are consistently selected as follows: $m_c = 5000$ kg, $k_c = 100000$ N/m, and $\xi_c = 0.15$. The accelerations at the 1/4, 1/2, and 3/4 spans of the beam and the deflection at the 1/2 span of the beam are calculated, and the results are shown in Figures 11 and 12.

The identification results are shown in Figure 13.

The ITDM based on the method of moments performs reasonably well in identifying the vehicle system model, with only a small error (~2.9%) in the single-point recognition when the vehicle travels to the midspan. This example demonstrates that the ITDM is also applicable to systems with a bridge-vehicle-coupled vibration effect.

5. Conclusions

In the present study, the authors explored the application of an improved time-domain identification method to a structure-vehicle system, which is a simplified kinetic model of the novel structure AERORail. The ability of the ITDM is verified under the moving loads and ¼ vehicle cases. The main conclusions are as follows:

(1) The acceleration curves demonstrate that the acceleration oscillation of the beam gradually increases as the moving load moves and gradually decreases after the load passes the midspan, and that the dynamic deflection increases to its maximum when the moving load moves near the midspan, after which it gradually returns to the equilibrium position and performs free damped vibration.

(2) The simplified dynamic numerical model of AERORail meets the requirements for carrying out

AERORail vibration calculations under the ML model. The ITDM based on the method of moments performs excellently in the identification of the ML during the simulation, and the feasibility of the algorithm is verified. Multipoint identification is more accurate than single-point identification, but the single-point identification results still have reliable accuracy.

(3) The difference between the load identification results and the original results is small at the start and end time points, and the error is approximately 4.72% at the middle time point. By adding the acceleration signal at the 1/4 span of the beam to the identification inputs, the identification result essentially coincides with the original moving load $p(t)$-t curve with high accuracy.

(4) The ITDM effectively reduces the matrix condition number and improves the matrix state, making the system of linear equations easier to solve. However, the order m of the Legendre polynomials should be selected appropriately since using an excessively high value of m does not substantially improve the calculation results.

(5) The results of numerical examples indicate that the ITDM has good accuracy. The calculation results are in almost perfect agreement with the true values, with errors between 2.9% and 4.72%, and satisfactory accuracy is achieved even in single-point signal identification.

The above conclusions are based on the estimated structural properties (stiffness, modes, and weight) of the AERORail and the ODE-based structure-vehicle model. Although the verification is limited to the numerical domain, it still shows the potential of the future application of the ITDM to the real AERORail and other civil engineering structures alike.

Data Availability

The data used to support the findings of this study are included in the article.

Conflicts of Interest

The authors declare that they have no conflicts of interest.

Acknowledgments

This research was supported by the National Natural Science Foundation of China (Grant nos. 50708072 and 51378385) and was supported by the Fundamental Research Funds for the Central Universities (Grant no. 22120180318).

References

[1] F. Li, "Structure form of pretension string rail structure and application prospect," in *Structures and Architecture*, P. J. S. Cruz, Ed., pp. 1546–1553, CRC Press, Boca Raton, FL, USA, 2010.

[2] L. S. Qin, "Discussion on new urban rail transit technology," *China Management Informatization*, vol. 20, no. 20, pp. 204-205, 2017.

[3] D. Y. Yang, "Challenges in urban transportation development under the new infrastructure construction: highlights of the 30th urban transportation development forum in China," *Urban Transport of China*, vol. 20, no. 05, pp. 106–121, 2022.

[4] F. Y. Li, P. F. Wu, and D. Liu, "Experimental study on the cable rigidness and static behaviors of AERORail structure," *Steel and Composite Structures*, vol. 12, no. 5, pp. 427–444, 2012.

[5] F. Y. Li, P. F. Wu, and D. J. Liu, "Application of virtual prototyping to simulation of vehicle-rail coupling of AERORail structure," *Journal of Tongji University*, vol. 40, no. 09, pp. 1287–1293, 2012.

[6] Y. C. Ji and Y. J. Kim, "State-of-the-art review of bridges under rail transit loading," vol. 172, no. 6, pp. 451–466, 2019.

[7] R. Liu, E. Dobriban, Z. Hou, and K. Qian, "Dynamic load identification for mechanical systems: a review," *Archives of Computational Methods in Engineering*, vol. 29, no. 2, pp. 831–863, 2021.

[8] P. Zhou, "Review of research and development status of dynamic load ldentification in TimeDomain," *Noise and Vibration Control*, vol. 34, no. 1, pp. 6–11, 2014.

[9] Z. Y. Li and C. F. Zhu, "Dynamic load identification method based on functional principle," *Foreign electronic measurement technology*, vol. 39, no. 10, pp. 51–54, 2020.

[10] Z. C. Yang and Y. Jia, "The identification method of dynamic load," *Advances in Mechanics*, vol. 45, no. 2, pp. 29–54, 2015.

[11] H. J. Yang, "Dynamic load identification based on deep convolution neural network," *Mechanical Systems and Signal Processing*, vol. 185, 2023.

[12] G. Wei and R. Zhuoyu, "Dynamic load identification based on piecewise fitting trend term and smooth curve," *Journal of Physics: Conference Series*, vol. 2364, no. 1, 2022.

[13] Y. Jing, "Study on the method of moving load identification based on strain influence line," *Applied Sciences*, vol. 11, no. 2, 2021.

[14] Y. Zhou, "Research on moving load identification based on measured acceleration and strain signals," *International Journal of Lifecycle Performance Engineering*, vol. 3, no. 3-4, 2019.

[15] H. Zhang, Y. H. Zhou, and L. W. Quan, "Identification of a moving mass on a beam bridge using piezoelectric sensor arrays," *Journal of Sound and Vibration*, vol. 491, 2020.

[16] E.-S. Hwang and A. S. Nowak, "Simulation of dynamic load for bridges," *Journal of Structural Engineering*, vol. 117, no. 5, pp. 1413–1434, 1991.

[17] T. L. Wang and D. Z. Huang, "Cable-stayed bridge vibration due to road surface roughness," *Journal of Structural Engineering*, vol. 118, no. 5, pp. 1354–1374, 1992.

[18] Y. B. Yang and B. H. Lin, "Vehicle-bridge interaction analysis by dynamic condensation method," *Journal of Structural Engineering*, vol. 121, no. 11, pp. 1636–1643, 1995.

[19] Y. B. Yang and J. D. Yau, "Vehicle-bridge interaction element for dynamic analysis," *Journal of Structural Engineering*, vol. 123, no. 11, pp. 1512–1518, 1997.

[20] G. H. Tan, G. H. Brameld, and D. P. Thambiratnam, "Development of an analytical model for treating bridge-vehicle interaction," *Engineering Structures*, vol. 20, no. 1-2, pp. 54–61, 1998.

[21] L. Kwasniewski, H. Li, J. Wekezer, and J. Malachowski, "Finite element analysis of vehicle–bridge interaction," *Finite*

Elements in Analysis and Design, vol. 42, no. 11, pp. 950–959, 2006.

[22] L. Ru, "Experimental study on indentification of moving vehicle loads on a bridge based on moments method," *Journal of Vibration and Shock*, vol. 26, no. 1, pp. 16–20, 2007.

[23] F. Fan, "Evaluating the dynamic response of the bridge-vehicle system considering random road roughness based on the moment method," *Advances in Civil Engineering*, vol. 2021, Article ID 9923592, 12 pages, 2021.

[24] V. Michael, B. Rune, and G. Christos, "Evaluating the effect of modelling errors in load identification using classical identification methods," *Shock and Vibration*, vol. 2019, Article ID 3148, 14 pages, 2019.

[25] W. C. Gibson, *The Method of Moments in Electromagnetics*, CRC Press, Boca Raton, FL, USA, 2007.

[26] F. Li, Z. Guo, Y. Cui, and P. Wu, "Dynamic load test and contact force analysis of the AERORail structure," *Applied Sciences*, vol. 13, 2023.

[27] R. J. Zhang, "Analysis of conditional number indexes for pathological problems in photogrammetry," *Journal of Wuhan University (Natural Science Edition)*, vol. 35, no. 3, pp. 308–312, 2010.